Progress In Electromagnetics Research B, Vol. 33, 21–44, 2011

SCALAR RADIATIVE TRANSFER IN DISCRETE MEDIA WITH RANDOM ORIENTED PROLATE SPHEROIDS PARTICLES

L. Bai, Z. S. Wu*, H. Y. Li, and T. Li

Physics Department, School of Science, Xidian University, Xi'an, Shaanxi 710071, China

Abstract—Monte Carlo scalar radiative transfer simulation of light scattering in plane parallel slab is not a simple problem, especially in the study of angular distribution of light intensity. Approximate phase function such as Henyey-Greenstein is often used to simulate the Mie phase function. But even for sphere particle this function is sometimes a poor approximation of real phase function. For a spheroids particle, the angular scattering characteristics cannot be approximated as *H-G* phase function with sufficient accuracy. In this paper, we study the transmission characteristics of light in parallel plane layer with randomly oriented prolate spheroids aerosol particles. Instead of using *H-G* phase function, we use sampling method to simulate real phase function of spheroid directly. A database of phase function with various scattering angle and azimuth angles for given spheroids aerosol particle is developed. The transmission characteristics calculated by scattering phase function sampling method and equivalent volume sphere *H-G* phase function method are compared. The effect of prolate spheroids particle size and form factor on optical transmission properties is analyzed. It is found that although the construction database of phase function takes a certain amount of computing time, for spheroid particles the sample phase function method, compared with the *H-G* phase function simulation method, can greatly improve the accuracy of transmittance calculation.

Received 29 April 2011, Accepted 5 July 2011, Scheduled 24 July 2011

* Corresponding author: Zhensen Wu (wuzhs@mail.xidian.edu.cn).

1. INTRODUCTION

The subject of wave propagation through discrete random media has substantial scientific interest due to a number of potentially applications in atmospheric optics, biomedicine, remote sensing and communication etc. [1–27].

There are various methods often used to solve the properties in random medium, such as Monte Carlo method, discrete ordinates method and two or four-flux method etc. Many studies on Monte Carlo simulation of photon propagation in various kinds of turbid media have been carried out [1–6]. Berrocal et al. used Monte Carlo method to calculate some typical aerosols with Mie scattering in the intermediate single-to-multiple scattering regime. And they developed a novel Monte Carlo code for modeling optical radiation propagation in inhomogeneous polydisperse scattering media [15–17]. The multiple scattering effect in Monte Carlo simulation was also discussed by Meglinski et al. [18]. In these related studies, particles are usually simplified as spheres. Volume-equivalent spherical particles and surface-equivalent spherical particles are often used as an approximation of non-spherical particle [1–3, 6, 9–19].

In the case of anisotropic random scattering media, both particle morphology and global orientation play an important role in transmittance properties. A few experiments have addressed light scattering in anisotropic random scattering media, such as nematic liquid crystals, or human tissues [5]. Moumini and Baravian discussed the anisotropic incoherent transport of light in media where prolate ellipsoids are oriented in the same direction [7]. Berdnik and Loiko [8] studied light scattering in media composed of spheroidal particles oriented along the same direction. Chang et al. [9] investigated the behavior of polarized light as it propagates through a medium of spheroidal scatters. They treated the multiple scattering effects by using the exactly scattering phase function, but the particles are small compared with incident wavelength. We have carried out some work on the transmittance properties of polydisperse spherical aerosol in UV to visible band and compared the H-G phase function simulation method with the random sample phase function simulation method [10, 11], but not including the case of a non-spherical case. In this paper, discussions about the transmittance properties of the media in which all particles are randomly oriented prolate ellipsoids aerosol are given. In the first part, we present the Monte Carlo method usually used for sphere particle, and in the second part, we discuss the interaction between a plane electromagnetic wave and a prolate ellipsoidal particle. Then we introduce the sample scattering phase function method instead of the

H-G scattering phase function simulation method. Finally, the effects of particle size and form factor on optical transmission properties with these different phase function simulation methods are analyzed.

2. MONTE CARLO SIMULATION METHOD

In all applications of the Monte Carlo method, a stochastic model should be constructed in which the expected value of a certain random variable (or of a combination of several variables) is equivalent to the value of a physical quantity to be determined [2]. In this paper, we use physical quantity transmissivity which can be determined by the statistical model.

2.1. Transport Theory of Wave Propagation in Random Particles

In transport theory, if polarization effect is not included, the equation of transfer without other emission source can be expressed as [12]

$$\frac{dI(\vec{r},\hat{s})}{ds} = -\rho\sigma_t I(\vec{r},\hat{s}) + \frac{\rho\sigma_t}{4\pi}\int_{4\pi} p(\hat{s},\hat{s}')I(\vec{r},\hat{s}')d\omega' \tag{1}$$

where $I(\vec{r},\ \hat{s})$ is the specific intensity at the point $\vec{r}$ with radiation along the direction $\hat{s}$; ρ is the number density of the media; $d\omega'$ is the solid angle; and $\sigma_t = \sigma_a + \sigma_s$, which is the extinction cross section. σ_a and σ_s are the absorption and scattering section, respectively. $p(\hat{s},\hat{s}')$ is the scattering phase function.

It is often convenient to divide the total intensity into two parts, reduced incident intensity I_{ri} and diffuse intensity I_d. They satisfy the equation as following respectively

$$\frac{dI_{ri}(\vec{r},\hat{s})}{ds} = -\rho\sigma_t I_{ri}(\vec{r},\hat{s}) \tag{2}$$

$$\frac{dI_d(\vec{r},\hat{s})}{ds} = -\rho\sigma_t I_d(\vec{r},\hat{s}) + \frac{\rho\sigma_t}{4\pi}\int_{4\pi} p(\hat{s},\hat{s}')I_d(\vec{r},\hat{s}')d\omega', \tag{3}$$

where $I_{ri} + I_d = I$. It is convenient to measure the distance in terms of a non-dimensional "optical thickness τ", which is defined by

$$\tau = \int \rho\sigma_t ds \tag{4}$$

For plane-parallel atmosphere, using the conception of optical thickness, Equation (3) becomes

$$I_d(\bar{\tau},\mu) = \int_0^{\tau_0} \exp\left[-\frac{\bar{\tau}-\tau'}{\mu}\right] J(\tau',\mu)\frac{d\tau'}{|\mu|} + I_{ri}(\bar{\tau},\mu), \tag{5}$$

where

$$J(\tau,\mu) = \frac{1}{2}\int_{-1}^{1} p(\mu,\mu')I_d(\tau,\mu')d\mu' \tag{6}$$

$$\bar{\tau} = \begin{cases} \tau_0 & \mu > 0 \\ 0 & \mu < 0 \end{cases} \tag{7}$$

$$I_{ri}(0,\mu) = 0(\mu < 0), \tag{8}$$

$$\mu = \cos\theta = \hat{s}\cdot\hat{s}' \tag{9}$$

The boundary condition could be expressed as

$$\begin{aligned} I_d(0,\mu) &= 0 \quad 0 \le \mu \le 1 \\ I_d(\tau_0,\mu) &= 0 \quad -1 \le \mu \le 0 \end{aligned} \tag{10}$$

Integral Equation (5) can be expressed as [28]

$$I(s) = I_{ri}(s) + \int I(s')K(s' \to s)ds' \tag{11}$$

And I_{ri} satisfied

$$\int I_{ri}(s)ds = \int_0^\infty e^{-\tau}d\tau \int\int_{4\pi} \delta(\mu-1)\delta(\varphi)d\mu d\varphi = 1$$

Equation (11) has the series solution

$$I(s) = \sum_{m=0}^{\infty} I_m(s) \tag{12}$$

where

$$\begin{aligned} I_0(s) &= I_{ri}(s) \\ I_1(s) &= \int I_0(s_0)K(s_0 \to s)ds_0 \\ &\cdots \\ I_m(s) &= \int I_{m-1}(s_{m-1})K(s_{m-1} \to s)ds_{m-1} \\ &= \int\ldots\int I_0(s_0)K(s_0 \to s_1)\ldots K(s_{m-1} \to s)ds_{m-1}\ldots ds_1 ds_0 \end{aligned} \tag{13}$$

Physically, $I_m(s)$ in Equation (13) means the emission density from the source at point P, through the mth time transmission and collision. Thus integral operator $\int K_\chi(s_{l-1} \to s_l)ds_{l-1}$ means that the particle experiences transmission and collision in disperse random medium once. We may rewrite Equation (13) in probability model, integral operator $\int K_\chi(s_{l-1} \to s_l)ds_{l-1}$ corresponding to conditional

probability $P(s_l|s_{l-1})$. Using statistical estimation method, we may obtain

$$P(s_{l+1}\,|s_l\,) = \exp\left[-\sigma_a\rho\,|(z_{l+1}-z_l)/\cos a_l|\right]\cdot\eta(h-z_l)\eta(z_l), \quad (14)$$

where a_l is the angle between the lth ($l = 1, 2, \ldots, m$) photon scattering direction and z axis. Exponential part means the lth photon scattering probability from point s_l to s_{l+1} without absorption. Analogously, integral operator $\int K_\chi(s_m \to s)ds_m$ is corresponding to state transition probability

$$P(s\,|s_m\,) = \exp\left[-\sigma_t\rho(h-z_m)/\cos a_m\right]\eta(\cos a_m), \quad (15)$$

Use weight function

$$W_{m+1} = W_m \exp\left[-\sigma_a\rho\,|(z_{m+1}-z_m)/\cos a_m|\right], \quad (16)$$

then, the direct transmission probability P_0 is

$$P_0 = W_0 \exp\left[-\sigma_t\rho(h-z_m)/\cos a_0\right], \quad (17)$$

Each photon is initially assigned a weight $W_0 = 1$, and a_0 is the angle between initial incident direction and z axis. So the statistical estimation of a photon transmissivity is

$$\begin{aligned} P_t = \sum_{m=0}^{\infty} P_m = \sum_{m=0}^{\infty} W_m \exp\left[-\sigma_t\rho(h-z_m)/\cos a_m\right]\cdot\eta(\cos a_m) \\ \cdot\prod_{l=1}^{m}\eta(h-z_l)\eta(z_l), \end{aligned} \quad (18)$$

where

$$\eta(x) = \begin{cases} 1 & x > 0 \\ 0 & x \le 0 \end{cases}$$

When N photons are generated, we may obtain the transmissivity T as

$$T = \frac{1}{N}\sum^{N} P_t. \quad (19)$$

2.2. Description of the Monte Carlo Simulation in Traditional Case

Monte Carlo algorithm is usually used to simulate the propagation properties of light in random media in traditional case (the particles in the layer is sphere case). Many related references discussed the Monte Carlo simulation method in this case. In [2, 3], Wang et al. pointed out that there are several parameters, which could completely describe the properties of the layer, namely the absorption coefficient $C_a = \rho\sigma_a$,

scattering coefficient $C_s = \rho\sigma_s$, anisotropy factor, and the thickness of the layer is h in z axis. If these parameters are determined, the total interaction coefficient $C_t = C_a + C_s$ is defined, so that its inverse C_t^{-1} is the mean free path between two consecutive interactions. The photon interacts with the medium in every step. For example, the photon is scattered and absorbed, and its left weight radio of the photon is defined by albedo C_s/C_t.

Usually, there are some typical steps in the simulation including:

1. photon initialization.
2. photon meeting the scatter in the media.
3. changing the direction of the photon.
4. judge the position of the photon.
5. sample the free path-length of the photon.
6. update the position of the photon.
7. update the absorption and the weight of the photon.
8. summarize all the photon update the transmittance.

Special attention should be paid to step 3. If the particle in the random media is sphere, usually used phase function is H-G phase function [13, 14]

$$p(\mu) = \frac{1 - g^2}{2[1 + g^2 - 2g\mu]^{3/2}} \tag{20}$$

where g is the asymmetry factor, and $\mu = \cos\theta = \hat{s} \cdot \hat{s}'$ is the cosine of scattering angle.

The probability distribution for the cosine of the deflection angle, $\cos\theta$, is described by the scattering function described above. The choice for $\cos\theta$ can be expressed as a function of the random number ξ.

$$\cos\theta = \begin{cases} \dfrac{1}{2g}\left[1 + g^2 - \left(\dfrac{1 - g^2}{1 - g + 2g\xi}\right)^2\right] & g \neq 0 \\ 2\xi - 1 & g = 0 \end{cases} \tag{21}$$

The azimuth angle for sphere particle, ψ, which is uniformly distributed over the interval 0 to 2π, is sampled as

$$\psi = 2\pi\xi \tag{22}$$

Once the deflection angle and azimuth angle are chosen, the new direction of the photon packet can be determined.

This scattering phase function simulation method is the most used one. But this function is often the poor approximations of real phase

function. Toublanc used an exact calculation phase functions for monodisperse particle [14]. Bai et al. simulated real phase function for some typical poly-disperse particles [10, 11]. These researches indicated that even for sphere particles H-G phase function is not a good approximation of real particles.

2.3. Description of the Propagation in Random Media with Spheroid Particles

For spheroid particle, the dependence of phase function on different scattering angles and azimuth angles is one defining feature of light scattering by spheroids rather than by sphere. In this paper, we use sample scattering phase function method to improve the simulation accuracy of scattering phase function of spheroid.

The physical model described in this paper is illuminated in Fig. 1. We suppose the transport of a plane wave perpendicularly incident on a plane parallel slab and that the layer is infinitely wide. The properties of the slab could be described by the following parameters: the thickness of the layer, refractive index, form factor and size of the spheroid particles in the layer.

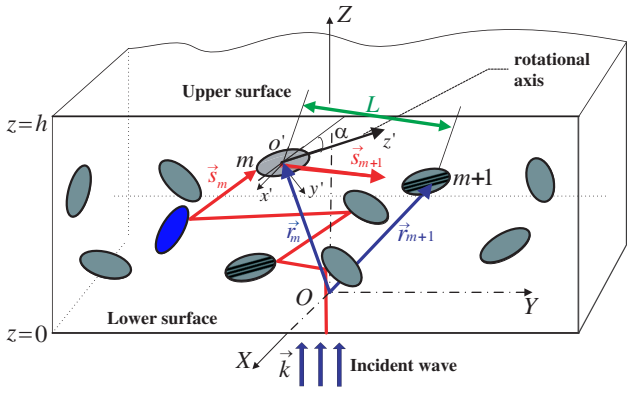

Figure 1. Scheme of photon propagation.

A succession of scattering events occurs when the photon hits rotational symmetry ellipsoidal particles.

To describe the propagation properties of photons in the medium, two coordinate systems are used in the simulation. We use a right-handed Cartesian-coordinate system with the orientation fixed in space as the laboratory coordinate system $OXYZ$.

In order to evaluate the scattering properties of the scattering particle, the local coordinate system $O'x'y'z'$ is defined as a moving

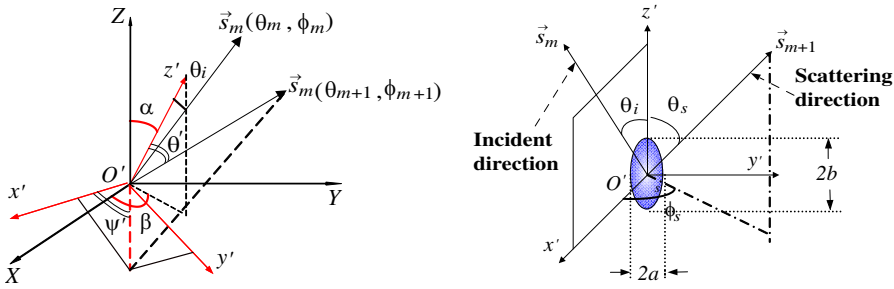

Figure 2. (a) Convention for the angle relationship. (b) Convention for the axes and the angles in local reference frame.

coordinate system. The origin O' is set as the center of the mth particle, and z' axis is set parallel to the axis of rotational symmetry.

The direction of z' axis relative to the laboratory coordinate frame $OXYZ$ can be specified by two angles (α, β), where $\alpha(0 \leq \alpha \leq \pi)$ is the elevation angle measured from the Z axis, and $\beta(0 \leq \beta \leq 2\pi)$ is the angle between the X axis and the projection of the $z\prime$ axis in the OXY plane, as illustrated in Fig. 2(a). The direction cosine of the z' axis in the laboratory coordinate $OXYZ$ is $(\sin\alpha\cos\beta,\ \sin\alpha\sin\beta,\ \cos\alpha)$. These angles $(\alpha,\ \beta)$ for every scatter are randomly selected to simulate the media with an ensemble of randomly oriented particles. They could be obtained by random sample method.

To create a random orientation, we could set the angle α satisfied $\sin\alpha = \xi$ and obtain the angle α and using $\beta = 2\pi\xi$ to obtain the angle β. This random sample for $(\alpha,\ \beta)$ is used only to simulate the randomly oriented directions of the spheroid in space.

When the photon scattered from the mth particle to the $m+1$th particle, in the laboratory coordinate frame $OXYZ$, the position vector and unit vector of the incident direction are denoted as $\vec{\mathbf{r}}_m$, $\vec{\mathbf{s}}_m$, $\vec{\mathbf{r}}_{m+1}$, $\vec{\mathbf{s}}_{m+1}$, respectively, as illustrated in Fig. 1. For convenience, the selection criterion of the x' axis is that: let the vector $\vec{\mathbf{s}}_m$ lie in the plane $O'x'z'$. Then determine the y' axis according to the right-handed principle (see Fig. 2(b)).

Denote the angle of the direction of the incident unit vector $\vec{s}_m$ in the laboratory coordinate frame $OXYZ$ system as $(\theta_m,\ \phi_m)$. As illustrated in Fig. 2(a), in the local coordinate frame $O'x'y'z'$ of the mth particle, the angle of incident wave θ_i satisfies the following equation:

$$\begin{aligned}\cos\theta_i \ = \ & \sin\theta_m\cos\phi_m\sin\alpha\cos\beta + \sin\theta_m\sin\phi_m\sin\alpha\sin\beta \\ & + \cos\theta_m\cos\alpha \end{aligned} \tag{23}$$

and the azimuth angle of the incident wave vector $\vec{\mathbf{s}}_m$ in local

coordinate frame $O'x'y'z'$ is $\phi_i = 0$ (as illustrated in Fig. 2(b)).

For sphere scatter in H-G phase function simulation method, the scattering angle could be selected according to Equation (21), and the azimuth angle could be determined by Equation (22). But in our simulation method the scattering angle θ_s and azimuth angle ϕ_s should be determined by sample method. When the direction of the incident wave in the $O'x'y'z'$ frame of the mth particle is determined, the scattering properties can be calculated by T-matrix. We can pre-calculate many scattering phase functions in different incident cases and store it as a scattering phase function database. This database is related with different incident angles, scattering angles, and azimuth angles (θ_i, $\phi_i = 0; \theta_s$, ϕ_s) in $O'x'y'z'$.

We could create a cumulative probability table of the normalized scattering phase function. If the random number $\xi(\xi \in (0, 1]$ is given, we could select a point along the range of probability sums, which then corresponds to a particular scattering angle. Once a ξ has been selected, the table is searched until [52]

$$\xi = \frac{\sum_{\theta_s=0}^{\theta_s} P(\theta_i; \theta_s, \phi_s)\Delta\Omega_s}{\sum_{\theta_s=0}^{180} P(\theta_i; \theta_s, \phi_s)\Delta\Omega_s} \tag{24}$$

where $P(\theta_i; \theta_s, \phi_s)$ is the phase function in the given angle of the incidence θ_i. $\Delta\Omega_s$ is the solid angle interval. With this method, the scattering angle θ_s is selected.

In a similar way as Equation (22), the azimuth angle ϕ_s could be determined. The direction of scattering (θ_s, ϕ_s) in the $O'x'y'z'$ frame of the mth particle is also the direction of incident of the $m + 1$th particle $\vec{\mathbf{s}}_{m+1}$.

In order to obtain the scattering direction of the mth particle in the laboratory coordinate, we should use transformation matrix $\mathbf{M}^{-1}$ from the local reference frame to the laboratory reference frame. Note that matrix $\mathbf{M}$ is from the laboratory reference frame to the local reference frame. The matrix $\mathbf{M}$ is given by

$$\mathbf{M} = \begin{bmatrix} \sin\beta & \cos\beta\cos\alpha & \cos\beta\sin\alpha \\ -\cos\beta & \sin\beta\cos\alpha & \sin\beta\sin\alpha \\ 0 & -\sin\alpha & \cos\alpha \end{bmatrix} \tag{25}$$

Then if the angle of (θ_s, ϕ_s) in the local reference frame is known, the direction of it in the laboratory reference frame could be obtained by angle rotation transform. More attention should be paid to that the unit vector $\vec{\mathbf{s}}_{m+1}(\theta_{m+1}, \phi_{m+1})$ in the $OXYZ$ corresponds to the

scattering direction (θ_s, ϕ_s) in $O'x'y'z'$. The scattering direction of the mth particle $\vec{\mathbf{s}}_{m+1}(\theta_{m+1}, \phi_{m+1})$ is also the incident direction of the $m+1$th particle in $OXYZ$.

Let the center of $m+1$th particle be the new O', and we can construct the new local reference frame $O'x'y'z'$. The incident direction of the $m+1$th particle in $OXYZ$ is then updated by $(\theta_{m+1}, \phi_{m+1})$.

Define the direction cosine of the unit vector $\vec{\mathbf{s}}_{m+1}$ in the $O'x'y'z'$ coordinate system as $\mu_1 = \sin\theta'\cos\psi'$, $\nu_1 = \sin\theta'\sin\psi'$, $w_1 = \cos\theta'$, where θ' is the angle between $\vec{\mathbf{s}}_{m+1}$ and the z' axis, and ψ' is the azimuth angle between the projection of $\vec{\mathbf{s}}_{m+1}$ in the $O'x'y'$ plane and the x' axis (as showed in Fig. 2(a)). The transformation matrix from the local reference frame to the laboratory reference frame can be expressed as

$$\begin{pmatrix} \mu \\ \nu \\ w \end{pmatrix} = \mathbf{M} \begin{pmatrix} \mu_1 \\ \nu_1 \\ w_1 \end{pmatrix} \tag{26}$$

where μ, ν, and w are the direction cosine of unit vector $\vec{\mathbf{s}}_{m+1}$ in the $OXYZ$ coordinate system. The photon position vector of the mth particle and the $m+1$th particle in the laboratory reference frame are $\vec{\mathbf{r}}_m$ and $\vec{\mathbf{r}}_{m+1}$, respectively (as showed in Fig. 1). We could set the coordinate of $\vec{\mathbf{r}}_m$ and $\vec{\mathbf{r}}_{m+1}$ in the laboratory reference frame as (X_m, Y_m, Z_m) and (X_{m+1}, Y_{m+1}, Z_{m+1}), then the relationship between them is

$$\begin{pmatrix} X_{m+1} \\ Y_{m+1} \\ Z_{m+1} \end{pmatrix} = \begin{pmatrix} X_m \\ Y_m \\ Z_m \end{pmatrix} + L \begin{pmatrix} \mu \\ \nu \\ w \end{pmatrix} \tag{27}$$

where $L = |\vec{\mathbf{r}}_{m+1} - \vec{\mathbf{r}}_m|$ is the mean free path, which could be determined by $L = -\ln\xi/C_t$. All the random numbers ξ used above are independent.

2.4. Scattering Properties of a Rotational Symmetry Spheroids Particle

The electromagnetic radiation and scattering properties of a rotational symmetry conducting/dielectric spheroid has been a hot area for many years [29–38]. And nowadays it still attracts interests of many scientists and engineers because of its wide applications.

Various calculation techniques have been proposed for the interaction between a plane electromagnetic wave and a single symmetry spheroid particle, such as the separation of variable method [36–38], shape perturbation method [39], discrete dipole approximation method [40] and T matrix method [33, 34, 41–51].

In this paper, we use T matrix method to construct the scattering phase function database of a spheroid. The T matrix method is a surface based method for homogenous particles commonly based on the extended boundary condition method (EBCM) that was introduced by Waterman [41] and has recently been reviewed by Mishchenko et al. [44, 45, 51]. Such an approach involves three parameters when determining the scattering properties of a given spheroid: size parameter $x = 2\pi r_v/\lambda$, refractive index m, and aspect ratio of the particle $\varepsilon = a/b$ (a and b are minor and major axes, respectively). It has been consistently observed that the accuracy and memory requirements strongly depend on particle size parameter, refractive indexes, and particle shape. As the size parameter and the refractive index of typical aerosol particles are not high, the T matrix method gives out reasonable results.

The T matrix code used in this study was developed by Mishchenko and available online as a Fortran code at the following url: www.giss.nasa.gov/$\sim$ crmin. The scattering properties of a rotational symmetry spheroid particle are calculated in particle local coordinate.

Figure 3 shows the graph of the variation of phase function $P(\theta_i, \phi_i = 0, \theta_s, \phi_s)$ of a spheroid particle with scattering angle θ_s in different incident angles. The incident azimuth angles and scattering azimuth angles in Fig. 3 are $\phi_i = 0^\circ$ and $\phi_s = 0^\circ$, respectively. The values are normalized by the area of axial cross section πab. Note that this phase function is only used to illustrate the relative scattering intensities by a spheroid. It is not the phase function used in the cumulative probability table.

Table 1. A comparison of the radiative transfer properties of different incident wavelengths.

λ/μm	r_v/μm	$\varepsilon = a/b$	T_1/s	T_{sample}/s	$T_{H\text{-}G}/s$
0.4	0.2	0.5	208	283	29
	0.1	0.5	23	66	5
	0.2	0.5	205	172	19
0.55	0.3	0.5	206	314	39
	0.2	0.6	22	176	23
	0.2	0.7	165	17	23
0.694	0.2	0.5	217	108	11

*where T_1 means the database calculate time, and T_{sample} and $T_{H\text{-}G}$ mean the calculation time of transfer by using the sample and the H-G phase function simulation method, respectively.

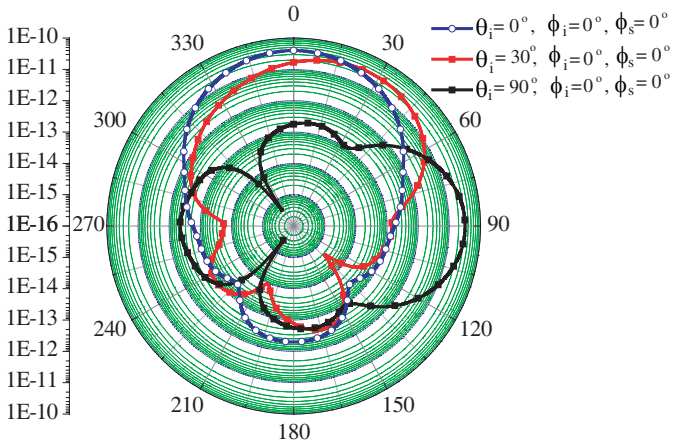

Figure 3. Phase function of a spheroid particle normalized by the area of axial cross section πab in different incident angles, with a refractive index $m = 1.385 + i9.9 \times 10^{-9}$, the wavelength of incident wave $\lambda = 0.4\,\mu\text{m}$, a volume-equivalent spherical radius $r_v = 0.2\,\mu\text{m}$, $a = r_v/\sqrt[3]{1/2} = 0.2/\sqrt[3]{1/2} \doteq 0.15874\,(\mu\text{m})$, and a form factor $\varepsilon = a/b = 0.5$.

3. RESULTS AND DISCUSSION

Table 1 shows a summary comparison result of computation time by using different phase function simulation methods. Different incident wavelengths, volume-equivalent spherical radius, and aspect ratio of the particle are calculated in Table 1. The simulation was developed in Fortran code, running on a standard computer (Intel core 2 duo processor, 1.86 GHz,500 G EMS memory). We chose 1000000 random numbers in the following calculation.

The refractive indexes of oceanic aerosol spheroid particles used in $0.4\,\mu\text{m}$, $0.5\,\mu\text{m}$ and $0.694\,\mu\text{m}$ incident wavelengths are $1.385 + i9.90 \times 10^{-9}$, $1.381 + i4.26 \times 10^{-9}$ and $1.376 + i5.04 \times 10^{-8}$, respectively [53].

Evaluation of the exact phase function requires slightly more computation time. The database calculation time is closely concerned with the radius and aspect ratio of the spheroid particle. If the aspect ratio of the particle is the same, the larger size is the parameter, the more time will be needed for the calculation. If the size parameter of the particle is the same, the smaller is the aspect ratio, the more calculation time will be needed too.

The total calculation time of the sample method is the summation of database calculation time t_1 and transmittance sample method

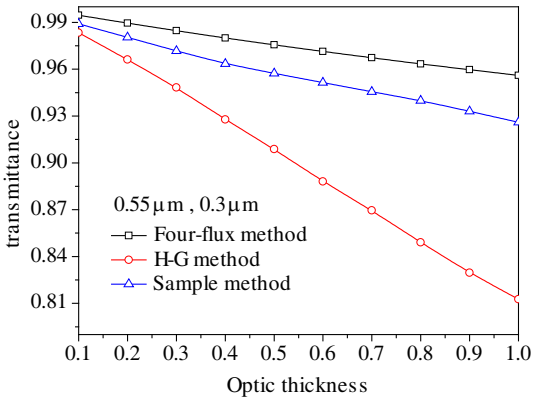

Figure 4. A graph of the variation of transmittance with optic thickness in different phase function simulation methods. (The volume equivalent spherical particle radius is 0.3 μm; the incident wavelength is 0.55 μm; the form factor of the spheroid is 0.5).

calculation time t_{sample}. It is almost 20 times longer than the *H-G* phase function simulation method. That is why the *H-G* phase function is the most used one. But for spheroid particle, the transmittance calculation results show big difference by using sample phase function method and *H-G* phase function method as illuminated in Fig. 4.

In Fig. 4, the plot of the variation of transmittance of oceanic prolate spheroid aerosol layer with optical thickness is presented. The transmittance results are compared with *H-G* scattering phase function simulation method and four-flux method. The incident wavelength is 0.55 μm. The volume equivalent spherical particle radius of random oriented prolate spheroids is 0.3 μm. And the form factor of the spheroid is 0.5. As can be seen from Fig. 4, the simulation results of sample method approach to that of four-flux method, but far away from the *H-G* phase function simulation results.

Figure 5 compares the transmittance properties of oceanic prolate spheroid aerosol layer by using *H-G* and sample phase function simulation method in different equivalent volume spherical particle radii. The incident wavelength is 0.55 μm. The form factor of the spheroid is $\varepsilon = 0.5$. With increased optic thickness, the transmittance decreases. And the transmittance also decreases as the equivalent volume spherical particle radius increases.

Figure 6 analyzes the effects of the incident wavelength on the transmittance by using *H-G* or sample phase function simulation

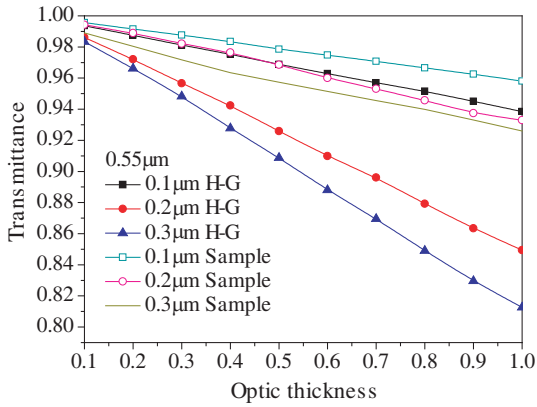

Figure 5. A graph of the variation of transmittance with optic thickness in different volume-equivalent spherical particle radii. (The incident wavelength is 0.55 μm, the form factor of the spheroid is 0.5 and the volume equivalent spherical particle radius is 0.1 μm, 0.2 μm and 0.3 μm respectively).

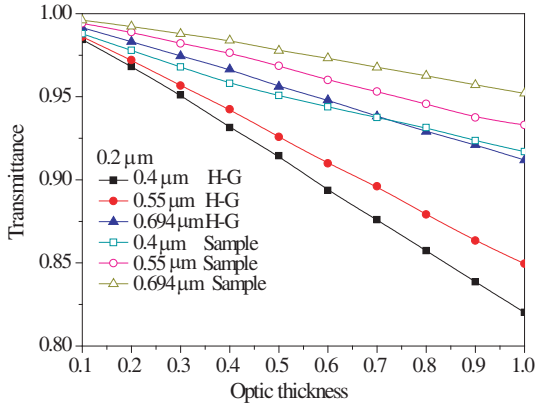

Figure 6. A graph of the variation of transmittance with optic thickness in different incident wavelengths. (The equivalent volume spherical particle radius is 0.2 μm, the form factor is $\varepsilon = 0.5$, the incident wavelength is 0.4 μm, 0.5 μm, and 0.694 μm respectively).

method. The parameter used in Fig. 6 is equivalent volume spherical particle radius 0.2 μm, and the form factor is $\varepsilon = 0.5$. The incident wavelengths are 0.4 μm, 0.55 μm and 0.694 μm, respectively.

As can be seen from Figs. 4–6, using the *H-G* phase function simulation method will underestimate the transmittance of the random layer with spheroid.

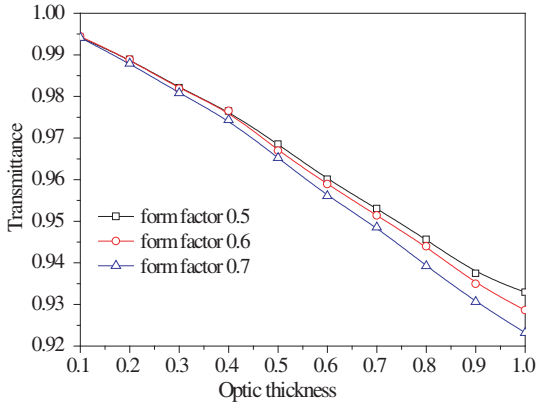

Figure 7. A comparison of transmittance of oceanic aerosol in different form factors. (The incident wavelength is 0.55 μm, the equivalent volume spherical particle radius is 0.2 μm and the form factor of the spheroid is 0.5, 0.6 and 0.7 respectively.

The sample scattering phase function method will greatly improve the accuracy of the transmittance.

Figure 7 calculates the transmittance of oceanic aerosol layer with different form factors. The incident wavelength is 0.55 μm; the equivalent volume spherical particle radius is 0.2 μm; the form factors of the spheroid in the calculation are 0.5, 0.6 and 0.7, respectively.

As can be seen from Fig. 7, with increased form factor, the transmittance of aerosol decreases because the average extinction coefficients of the particle increase as the form factor increases. But as the variation of the average extinction coefficients is very small, the difference of transmittance of oceanic aerosol in different form factors is not obvious. At the same time, the optic thickness of the plane parallel atmosphere is usually very small. The commonly encountered optic thickness of aerosol is in the range of 0.1–1. We can see from Fig. 7 that when the optic thickness is 1.0, the relative error of the transmittance with different spheroid particles form factors is obviously increased.

We should pay more attention to the multiple scattering occurring when the photon propagation in the random layer.

The multiple scattering that we defined in this paper is the times photon collided with spheroid aerosol particle in the layer. If the photon collided with the spheroid particle two times or more in the layer, we sum them together as the multiple scattering times. The ratio of multiple scattering times to the total scattering times is defined as

the percentage of multiple scattering.

Figure 8 shows the percentage of multiple scattering with optic thickness in different equivalent volume spherical particle radii. The equivalent volume spherical particle radii are 0.1 μm, 0.2 μm, and 0.3 μm, respectively. The other parameters used in Fig. 8 are the same as those in Fig. 5.

It can be found that the percentage of multiple scattering will increase while the optic thickness is increased. And when the equivalent volume spherical radius of spheroid is small compared with the incident wavelength, as illuminated in Fig. 8, 0.1 μm case, the percentage of multiple scattering is almost not sensitive varying with optic thickness. But when the equivalent volume spherical radius of spheroid is 0.3 μm, the percentage of multiple scattering rises fast.

Another example is illuminated in Fig. 9. In Fig. 9, the percentage of multiple scattering with optic thickness in different incident wavelengths is presented. The equivalent volume spherical particle radius is 0.2 μm, and the form factor is $\varepsilon = 0.5$. The incident wavelengths are 0.4 μm, 0.55 μm, and 0.694 μm, respectively. And when the incident wavelength is 0.694 μm, the volume spherical particle radius 0.2 μm is a relative small particles. We could obtain similar results in Fig. 8.

We define the relative error of transmittance as $(t_x(\tau) - t_{HG}(\tau))/t_{HG}(\tau)$, where $t_x(\tau)$ and $t_{HG}(\tau)$ stand for transmittance calculation results obtained from sample method and H-G phase

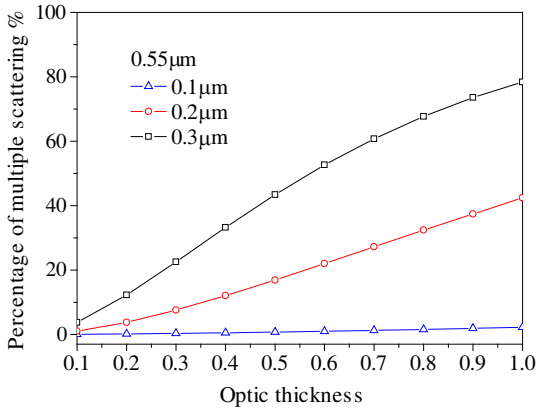

Figure 8. The percentage of multiple scattering with optic thickness in different equivalent volume spherical particle radii. (The incident wavelength is 0.55 μm, the equivalent volume spherical particle radius is 0.1 μm, 0.2 μm and 0.3 μm respectively. The form factor is $\varepsilon = 0.5$).

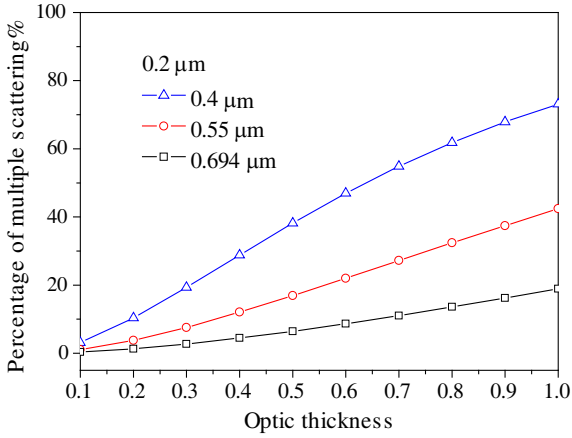

Figure 9. The percentage of multiple scattering with optic thickness in different wavelengths. (The equivalent volume spherical particle radius is 0.2 μm, the form factor is $\varepsilon = 0.5$. The incident wavelength is 0.4 μm, 0.55 μm and 0.694 μm respectively.

function simulation method, respectively.

We can use this quantity to express the difference of transmittance caused by different scattering phase function simulation methods.

Figure 10 represents relative error between transmittance of oceanic aerosol and and the transmittance of equivalent spherical particle in different equivalent spherical particle radii

Figure 10 leads us to a conclusion that the relative error of transmittance increases with increasing optical thickness.

Comparing with Figs. 8 and 10, we can see that the relative error is related to the percentage of multiple scattering. As the equivalent volume spherical particle radius is 0.2 μm for example, when the optic thickness is 0.1, the percentage of multiple scattering as showed in Fig. 8 is only about 5%. The relative error is only about 1%. But when the optic thickness is increased to 1.0, the percentage of multiple scattering is near 40%. The relative error approaches to about 8%.

It can be found that the relative error relates to the percentage of multiple scattering. If the percentage of multiple scattering increases, the relative error of transmittance increases too.

As it also can be seen from Fig. 10 that with increased equivalent volume particle radius, the relative errors of transmittance increase.

Figure 11 presences the comparison results of the relative error of transmittance with two types of phase functions simulation methods in different form factors. The incident wavelength is 0.55 μm; the equivalent volume spherical particle radius is 0.2 μm; and the form

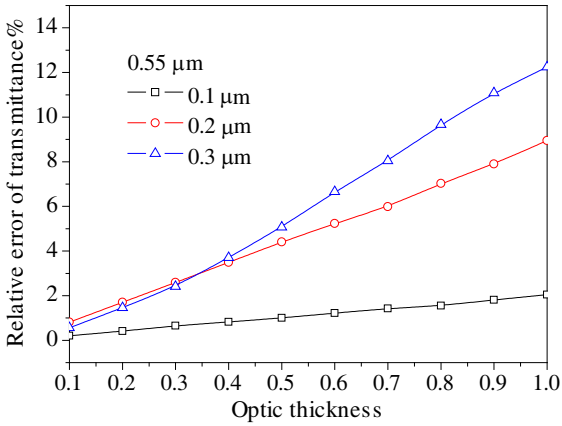

Figure 10. The relative error between transmittance of oceanic aerosol with optical thickness in different equivalent volume spherical particle radii. (The incident wavelength is 0.55 μm, the equivalent volume spherical particle radius is 0.1 μm, 0.2 μm and 0.3 μm respectively. The form factor is $\varepsilon = 0.5$).

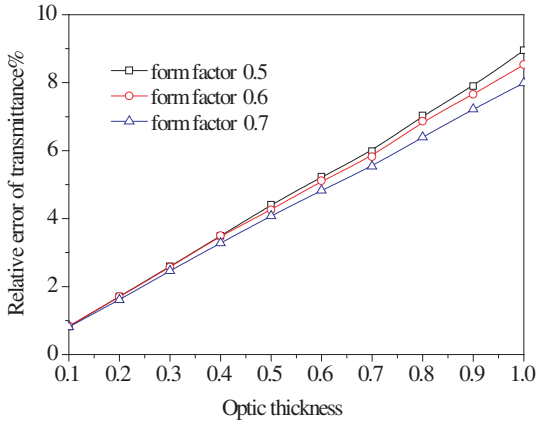

Figure 11. The relative error with optical thickness of oceanic aerosol in different form factors. (The incident wavelength is 0.55 μm the equivalent volume spherical particle radius is 0.2 μm and the form factor is 0.5, 0.6 and 0.7 respectively).

factors are 0.5, 0.6 and 0.7, respectively.

A form factor is defined as $\varepsilon = a/b$, where a is the minor axis of an ellipsoidal particle and b is the major axis of the spheroid particle. So the scattering characteristics of prolate spheroids aerosol would became

closer to spherical particles as the form factor increased from 0.5 to 0.7. And the transmittance properties of the layer with random oriented spheroid would be near the transmittance properties of aerosol particles composed by spherical particles.

4. CONCLUSION

In this paper, we discuss the transmittance characteristics of light in media where prolate spheroids are oriented in random direction. In these media, light transport is investigated by using Monte Carlo simulations method where the effects of particle (such as the equivalent volume spherical particle radius, the incident wave length and the form factor etc.) on optical properties are explored. A database of phase function of prolate spheroids aerosol particles is constructed. Calculation times of phase function database sample method and *H-G* phase function simulation method are presented.

It can be found that if the percentage of multiple scattering increases, the phase function simulation method should be selected more carefully. Commonly used *H-G* phase function approximation method is time saving, but it only fits for single scattering dominating case. If the percentage of multiple scattering increases or the optic thickness is large, more precise phase function simulation method would be needed. Otherwise, the transmittance would get more relative error. The calculation time is related to the equivalent volume spherical particle radius, extinction coefficients, form factor and incident wavelength. In the same form factor, the larger is the particle size parameter, the longer calculation time would be needed. If the size parameter of the particle is the same, the smaller is the form factor, the longer is the calculation time. And the relative error between phase function database simulation method and *H-G* phase function simulation method has close relationship with the percentage of multiple scattering. When the multiple scattering is dominated, the relative error would become larger.

ACKNOWLEDGMENT

The authors would like to thank the anonymous reviewers for their invaluable comments and suggestions, which lead to great improvement of our manuscript. Thanks are also extended to M. I. Mishchenko for providing the Fortran code of spheroid used in support of this research and the National Natural Science Foundation of China (No. 60971065) and the Fundamental Research Funds for the Central Universities.

REFERENCES

1. Plass, G. N. and G. W. Kattawar, "Monte Carlo calculations of light scattering from clouds," *Appl. Opt.*, Vol. 7, 415–419, 1968.
2. Wang, L. H., S. L. Jacques, and L. Q. Zheng, "MCML-Monte Carlo modeling of light transport in multi-layered tissues," *Computer Methods and Programs in Biomedicine*, Vol. 47, 131–146, 1995.
3. Wang, L. H., S. L. Jacques, and L. Q. Zheng, "CONV — Convolution for responses to a finite diameter photon beam incident on multilayered tissues," *Computer Methods and Programs in Biomedicine*, Vol. 54, 141–150, 1997.
4. Balbas, E. M. and P. J. French, "Shape based Monte Carlo code for light transport in complex heterogeneous tissues," *Opt. Express*, Vol. 15, 14086–14098, 2007.
5. Kienle, A., L. Lilge, M. S. Patterson, R. Hibst, R. Steiner, and B. C. Wilson, "Spatially resolved absolute diffuse reflectance measurements for noninvasive determination of the optical scattering and absorption coefficients of biological tissue," *Appl. Opt.*, Vol. 35, 2304–2314, 1996.
6. Prahl, S. A., M. Keijzer, S. L. Jacques, and A. J. Welch, "A Monte Carlo model of light propagation in tissue," *Proc. SPIE*, 102–111, 1989.
7. Moumini, N. and C. Baravian, "Incoherent light transport in anisotropic media: Form factor influence for oriented prolate ellipsoids," *J. Quant. Spectrosc. Radiat. Transfer*, Vol. 110, 1545–1565, 2009.
8. Berdnik, V. and V. Loiko, "Radiative transfer in a layer with oriented spheroidal particles," *J. Quant. Spectrosc. Radiat. Transfer*, Vol. 63, 369–382, 1999.
9. Chang, P. C. Y., J. G. Walker, E. Jakeman, and K. I. Hopcraft, "Polarization properties of light multiply scattered by non-spherical Rayleigh particles," *Waves Random Media*, Vol. 9, 415–426, 1999.
10. Bai, L., S. Q. Tang, Z. S. Wu, P. H. Xie, and S. M. Wang, "Study of random sample scattering phase functions of polydisperse atmospheric aerosol in ultraviolet band," *Acta Physica Sinica*, Vol. 59, 1749–1755, 2010.
11. Bai, L., Z. S. Wu, S. Q. Tang, M. Li, P. H. Xie, and S. M. Wang, "Study on phase function in Monte Carlo transmission characteristics of poly-disperse aerosol," *Optical Engineering*, Vol. 50, 016002, 1–8, 2011.

12. Ishimaru, A., *Wave Propagation and Scattering in Random Media*, Academic, New York, 1978.
13. Henyey, L. C. and J. L. Greenstein, "Diffuse radiation in the galaxy," *Astrophys. J.*, Vol. 93, 70–83, 1941.
14. Toublanc, D., "Henyey-Greenstein and Mie phase functions in Monte Carlo radiative transfer computations," *Appl. Opt.*, Vol. 35, 3270–3274, 1996.
15. Berrocal, E., D. Y. Churmakov, V. P. Romanov, M. C. Jermy, and I. V. Meglinski, "Crossed source detector geometry for novel spray diagnostic: Monte Carlo simulation and analytical results," *Appl. Opt.*, Vol. 44, 2519–2529, 2005.
16. Berrocal, E. and I. V. Meglinski, "New model for light propagation in highly inhomogeneous poly disperse turbid media with applications in sprays diagnostics," *Opt. Express*, Vol. 13, 9181–9195, 2005.
17. Berrocal, E., D. L. Sedarsky, M. E. Paciaroni, I. V. Meglinski, and M. A. Linne, "Laser light scattering in turbid media Part I: Experimental and simulated results for the spatial intensity distribution," *Opt. Express*, Vol. 15, 10649–10665, 2007.
18. Meglinski, I. V., V. L. Kuzmin, D. Y. Churmakov, and D. A. Greenhalgh, "Monte Carlo simulation of coherent effects in multiple scattering," *Proc. R. Soc. A*, Vol. 461, 43–53, 2005.
19. Blaunstein, N., "Theoretical aspects of wave propagation in random media based on quanty and statistical field theory," *Progress In Electromagnetics Research*, Vol. 47, 135–191, 2004.
20. Tateiba, M. and Z. Q. Meng, "Wave scattering from conducting bodies embedded in random media — Theory and numerical results," *Progress In Electromagnetics Research*, Vol. 14, 317–361, 1996.
21. Barabanenkov, Y. N., L. M. Zurk, and M. Y. Barabanenkov, "Single scattering and diffusion approximations for modified radiative transfer theory of wave multiple scattering in dense media near resonance," *Progress In Electromagnetics Research*, Vol. 15, 27–61, 1997.
22. Zhang, Y. J., A. Bauer, and E. P. Li, "A novel coupled T-matrix and microwave network approach for multiple scattering from parallel semicircular channels with eccentric cylindrical inclusions," *Progress In Electromagnetics Research*, Vol. 53, 109–133, 2005.
23. Zhang, Y. J. and E. P. Li, "Fast multipole accelerated scattering matrix method for multiple scattering of a large number of

cylinders," *Progress In Electromagnetics Research*, Vol. 72, 105–126, 2007.

24. Setijadi, E., A. Matsushima, N. Tanaka, and G. Hendrantoro "Effect of temperature and multiple scattering on rain attenuation of electromagnetic waves by a simple spherical model," *Progress In Electromagnetics Research*, Vol. 99, 339–354, 2009.
25. Wang, L., J. A. Kong, K. H. Ding, T. L. Toan, F. R. Baillarin, and N. Floury, "Electromagetic scattering model for rice canopy based on Monte Carlo simulation," *Progress In Electromagnetics Research*, Vol. 52, 153–171, 2005.
26. Gao, D. and L. Gao, "Tunable lateral shift through nonlinear composites of nonspherical particles," *Progress In Electromagnetics Research*, Vol. 99, 273–287, 2009.
27. Setijadi, E., A. Matsushima, N. Tanaka, and G. Hendrantoro, "Effect of temperature and multiple scattering on rain attenuation of electromagnetic waves by a simple spherical model," *Progress In Electromagnetics Research*, Vol. 99, 339–354, 2009.
28. Wu, Z. S. and Y. P. Wang, "Study of scattering of plane wave though discrete random medium by direct analogue and statistical estimation," *Acta Physica Sinica*, Vol. 37, 698–704, 1988 (in Chinese).
29. Asano, S. and G. Yamamoto, "Light scattering by a spheroidal particle," *Appl. Opt.*, Vol. 14, 29–49, 1975.
30. Asano, S., "Light scattering properties of spheroidal particles," *Appl. Opt.*, Vol. 18, 712–723, 1979.
31. Moffatt, D. L. and E. M. Kennaugh, "The axial echo area of a perfectly conducting prolate spheroid," *IEEE Trans. Antennas Propagat.*, Vol. 13, 401–409, 1965.
32. Sinha, B. P. and R. H. MacPhie, "Electromagnetic scattering by prolate spheroids for plane waves with arbitrary polarization and angle of incidence," *Radio Sci.*, Vol. 12, 171–184, 1977.
33. Mishchenko, M. I., "Light scattering by randomly oriented axially symmetric particles," *J. Opt. Soc. Am. A*, Vol. 8, 871–882, 1991.
34. Mishchenko, M. I., J. W. Hovenier, and L. D. Travis, *Light Scattering by Nonspherical Particles: Theory, Measurements, and Applications*, Academic, San Diego, Calif., 2000.
35. Li, L. W., T. S. Yeo, and M.-S. Leong, "Bistatic scattering and backscattering of electromagnetic waves by conducting and coated dielectric spheroids: A new analysis using mathematica package," *Progress In Electromagnetics Research*, Vol. 31, 225–245, 2001.
36. Li, L. W., M. S. Yeo, and M. S. Leong, "EM fields inside a prolate

spheroid due to a thin circular loop: A higher-order perturbation approach," *Progress In Electromagnetics Research*, Vol. 34, 219–252, 2001.

37. Li, L. W., X. K. Kang, and M.-S. Leong, *Spheroidal Wave Functions in Electromagnetic Theory*, Wiley, New York, 2002.
38. Han, Y. P. and Z. S. Wu, "Scattering of a spheroidal particle illuminated by a Gaussian beam," *Appl. Opt.*, Vol. 40, 2501–2509, 2001.
39. Kotsis, A. D. and J. A. Roumeliotis, "Electromagnetic scattering by a metallic spheroid using shape perturbation method," *Progress In Electromagnetics Research*, Vol. 67, 113–134, 2007.
40. Draine, B. T. and P. J. Flatau, "Discrete-dipole approximation for scattering calculations," *J. Opt. Soc. Am. A*, Vol. 11, 1491–1499, 1994.
41. Waterman, P. C., "Symmetry, unitarity, and geometry in electromagnetic scattering," *Phys. Rev. D*, Vol. 3, 825–839, 1971.
42. Mishchenko, M. I., "T-matrix theory of electromagnetic scattering by particles and its applications: A comprehensive reference database," *J. Quant. Spectrosc. Radiat. Transfer*, Vol. 88, 357–406, 2004.
43. Mishchenko, M. I., G. Videen, V. A. Babenko, N. G. Khlebtsov, and T. Wriedt, "Comprehensive T-matrix reference database: A 2004–2006 update," *J. Quant. Spectrosc. Radiat. Transfer*, Vol. 106, 304–324, 2007.
44. Mishchenko, M. I., G. Videen, N. G. Khlebtsov, T. Wriedt, and N. T. Zakharova, " Comprehensive T-matrix reference database: A 2006–2007 update," *J. Quant. Spectrosc. Radiat. Transfer*, Vol. 109, 1447–1460, 2008.
45. Mishchenko, M. I., "Capabilities and limitations of a current Fortran implementation of the T-matrix method for randomly oriented, rotationally symmetric scatterers," *J. Quant. Spectrosc. Radiat. Transfer*, Vol. 60, 309–324, 1998.
46. Doicu, A. and T. Wriedt, "Null-field method with discrete sources to electromagnetic scattering from composite objects," *Opt. Commun.*, Vol. 190, 13–17, 2001.
47. Doicu, A., "Null-field method to electromagnetic scattering from uniaxial anisotropic particles," *Opt. Commun.*, Vol. 218, 11–17, 2003.
48. Chew, W. C., Y. M. Wang, and L. Gürel, "Recursive algorithm for wave-scattering using windowed addition theorem," *Journal of Electromagnetic Waves and Applications*, Vol. 6, No. 11, 1537–

1560, 1992.

49. Chew, W. C., "Recurrence relations for three-dimensional scalar addition theorem," *Journal of Electromagnetic Waves and Applications*, Vol. 6, No. 1–6, 133–142, 1992.
50. Chew, W. C. and Y. M. Wang, "Efficient ways to compute the vector addition theorem," *Journal of Electromagnetic Waves and Applications*, Vol. 7, No. 5, 651–665, 1993.
51. Mishchenko, M. I., L. D. Travis, and D. W. Mackowski, "T-matrix computations of light scattering by nonspherical particles: A review," *J. Quant. Spectrosc. Radiat. Transfer*, Vol. 55, 535–575, 1996.
52. Bates, D. E. and J. N. Porter, "AO3D: A Monte Carlo code for modeling of environmental light propagation," *J. Quant. Spectrosc. Radiat. Transfer*, Vol. 109, 1802–1824, 2008.
53. Levoni, C., M. Cervino, R. Guzzi, and F. Torricella, "Atmospheric aerosol optical properties: A database of radiative characteristics for different components and classes," *Appl. Opt.*, Vol. 36, 8031–8041, 1997.